Active Damping Control Strategy of Matrix Converter via Modifying Input Reference Currents

Jiaxing Lei, *Student Member, IEEE*, Bo Zhou, Xianhui Qin, Jiadan Wei, *Member, IEEE*, and Jinliang Bian

***Abstract*—The matrix converter (MC) with an *LC* filter at source side suffers from system instability, thereby requiring damping control. To improve system stability, this paper proposes a novel active damping control strategy. First, the method of generating space vector modulation signals is improved, in order to make the amplitude and phase angle of input currents directly controllable without affecting the priority of output voltage control. Then, the proposed strategy, which is realized by injecting damping signals into input reference currents, is presented. In this way, the proposed strategy can suppress the oscillations in source currents directly. Besides, it is effective with source voltages or capacitor voltages sampled for modulation, regardless of the operation mode of MC. Furthermore, it is applicable to most of existing modulation algorithms. Finally, experimental results of four-quadrant operation on a 2.4-kW prototype illustrate that, under the condition of the same parameters, the proposed active damping control strategy performs better than passive damping control in filtering and the same in damping at source side, without sacrificing the driving performance at output side.**

***Index Terms*—Active damping control, input currents control, *LC* filter, matrix converter (MC).**

I. Introduction

MATRIX Converter (MC) has attracted intensive attentions and is often suggested as a potential alternative topology to back-to-back converter for its numerous merits, such as more compact size, lighter weight, and longer lifetime [1]–[4]. MC has two subtypes: conventional matrix converter (CMC) and indirect matrix converter (IMC). Although CMC and IMC differ from each other in the aspects of topology, commutation strategy, power loss, and so on, they can achieve the same functionality [1], [2]. Many researchers have been focusing on the control strategies, modulation algorithms, extended topologies, and applications of CMC and IMC [5]–[13].

Essentially, all kinds of MCs transfer power between a voltage source and a current source. The voltage source is usually taken as the input, with a *LC* filter required to obtain high-quality source currents and assist the commutation of power switches. Since the filter is likely to give rise to a resonant mode, damping control is demanded to suppress the oscillations. Paralleling a resistor with the filter inductor is a general passive damping method [14], which is easy to implement. However, current flows through the resistor, leading to power loss and less attenuation around switching frequency [15]. Moreover, in some specific applications, such as the situation of a generator source where stator inductance acts as the filter inductor, the resistor cannot be installed. One solution for these problems is active damping control, which could suppress the oscillations effectively through algorithms without a physical resistor.

Some achievements have been made in the area of active damping control for MC [16]–[23]. A general constructive method to stabilize MC was proposed by [16], which demonstrated that increasing the input admittances to positive values could improve the system small-signal stability. It has been the most comprehensive study so far and helps to explain many existing active damping methods, such as those in [17]–[19], which smooth the amplitude and/or phase of capacitor voltages with low-pass filters. Rivera *et al.* [20], [21] used dc blockers to detect the oscillation components and injected them into the output reference currents, realizing active damping control based on predictive current control strategy. The idea in [20] and [21] came from emulating a damping resistor in parallel with the filtering capacitor. In the situation of MC with a generator input, [22] investigated the active damping control strategy by applying feedback control of per-unit source currents, which showed good damping performance when configured with appropriate PID parameters. Sato *et al.* [23] proposed another active damping method realized by adding the filtered capacitor voltages into input reference currents, which were calculated based on instantaneous power theory with input active and reactive power set to 1 and 0, respectively. A special modulation algorithm presented in [24], which was claimed to enable independent control of input currents and output voltages, was applied to the MC studied in [22] and [23].

The achievements in active damping control for MC are significant, but there are still some improvements to be made. On one hand, most of existing methods involve filtered capacitor voltages in system control strategy and/or converter modulation algorithm, indirectly suppressing the oscillations in source currents. As the oscillations are often excited by the harmonics in input currents [21], controlling input currents is a more direct and effective active damping way, such as those in [22] and [23]. However, in [22] and [23], it is assumed that the input currents should be independently controlled, which is a strict constraint. It is generally considered that [1], [2], as output voltage control is preferential, only the phase angle of input currents can be

Manuscript received June 24, 2014; revised September 17, 2014; accepted October 21, 2014. Date of publication October 29, 2014; date of current version April 15, 2015. This work was supported in part by National Natural Science Foundation of China under Grant 51177069, by Jiangsu Province University Outstanding Science and Technology Innovation Team, by Funding of Jiangsu Innovation Program for Graduate Education under Grant KYLX_0269, and by the Fundamental Research Funds for the Central Universities. Recommended for publication by Associate Editor Dr. L. Chang.

The authors are with Jiangsu Key Laboratory of New Energy Generation and Power Conversion, College of Automation Engineering, Nanjing University of Aeronautics and Astronautics, Nanjing 210016, China (e-mail: ljxnuaa@nuaa.edu.cn; zhoubo@nuaa.edu.cn; qinxianhui.nuaa@gmail.com; weijiadan@nuaa.edu.cn; bjlnuaa@nuaa.edu.cn).

Color versions of one or more of the figures in this paper are available online at http://ieeexplore.ieee.org.

Digital Object Identifier 10.1109/TPEL.2014.2365578

predetermined, but the amplitude cannot for the reason that it has to be adjusted passively with output currents. This results in the inability to control the input currents independently. Actually, the method in [22] was later proved to interfere with closed-loop control of output current by the Haruna and Itoh in [25]. Besides, most of existing algorithms are considered not feasible for such methods due to the strict constraint [16].

On the other hand, although the passive damping control has some drawbacks, it is still widely used in practice [3], [26], due to its good damping performance in steady state and dynamic process. Most of the existing active damping control strategies can improve the small-signal stability of MC. But few strategies have been proved to have comparable damping performance with passive damping control. Actually, digital filters are widely used in existing methods, leading to compromises between stability and dynamic performance [16], and limited range of parameters adjustment [21]. Besides, as stated in [16], the general constructive methods in motoring mode and generating mode of MC are in conflict, while passive damping control are suitable for both modes. As a result, most of existing methods can hardly rival passive damping control in the respect of damping performance.

Aiming at these two aspects, this paper proposes an active damping control strategy via modifying input reference currents, which features comparable damping performance with passive damping control, suitability for most of existing modulation algorithms and no influence on the priority of output control. This paper is organized as follows. In Section II, a new method to generate modulation signals is introduced, in order to directly control the input current without affecting output voltage control. On this basis, the principle and realization of the proposed strategy are presented in Section III. Section IV makes some discussions about the applicability of the proposed strategy for the case with capacitor voltages sampled for modulation and for most of existing modulation algorithms. Its advantages over previous methods and the drawbacks are both discussed. In Section V, experiments are carried out on a 2.4-kW IMC-fed permanent magnet synchronous motor (PMSM) drive prototype, in order to verify the feasibility and validity of the proposed strategy. In Section VI, the conclusions of this paper are drawn.

II. New Method to Generate Modulation Signals

This section takes the widely studied space vector modulation (SVM) algorithm as an example to show how to directly control input currents without affecting the priority of output voltage control. Based on this, the proposed strategy is realized completely in Section III. But the proposed strategy does not restrict to SVM and is proved to be suitable for most of existing algorithms.

A. MC Model

No major differences exist in the mathematical models of CMC and IMC and, thus, this paper select IMC for study without loss of generality. Fig. 1 shows the topology of a IMC-fed PMSM drive system. The IMC is composed of a current source rectifier (CSR) and a voltage source inverter (VSI). Similarly,

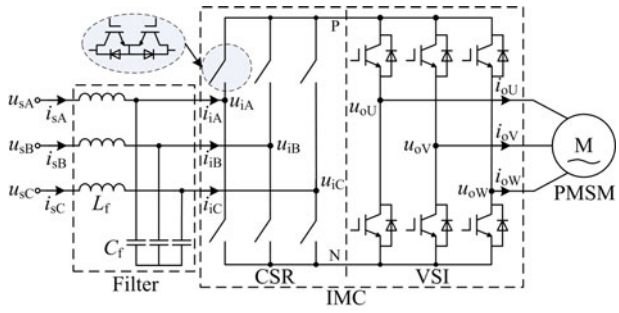

Fig. 1. IMC-PMSM drive system.

CMC can be considered as the combination of a virtual CSR and a virtual VSI [27]. Power source is connected to the input of CSR through an *LC* filter. PMSM is located at the output of VSI.

According to [27], the three phase input currents of MC modulated by SVM are

$$\begin{bmatrix} i_{\mathrm{iA}} \\ i_{\mathrm{iB}} \\ i_{\mathrm{iC}} \end{bmatrix} = m_{\mathrm{c}} \cdot \begin{bmatrix} \cos\theta_{\mathrm{ii}} \\ \cos\left(\theta_{\mathrm{ii}} - 2\pi/3\right) \\ \cos\left(\theta_{\mathrm{ii}} + 2\pi/3\right) \end{bmatrix} \cdot i_{\mathrm{dc}} = T_{\mathrm{CSR}} i_{\mathrm{dc}} \quad (1)$$

where i_{iA}, i_{iB}, and i_{iC} are the low-frequency components of input current (unless otherwise stated, all the symbols in this paper represent the low- frequency components); T_{CSR} is the transfer function matrix of CSR and is called the modulation signals in this paper because it contains all the information required by SVM of CSR; i_{dc} is the dc-link current; θ_{ii} is the (reference) phase angle of input current vector; m_c is the current modulation index of CSR, denoted as the ratio of the input current amplitude i_{im} and dc-link current i_{dc}

$$m_{\mathrm{c}} = i_{\mathrm{im}}/i_{\mathrm{dc}}. \quad (2)$$

Analogously, the three-phase output voltages can be expressed as [27]

$$\begin{bmatrix} u_{\mathrm{oU}} \\ u_{\mathrm{oV}} \\ u_{\mathrm{oW}} \end{bmatrix} = m_{\mathrm{v}} \cdot \begin{bmatrix} \cos\theta_{\mathrm{ou}} \\ \cos\left(\theta_{\mathrm{ou}} - 2\pi/3\right) \\ \cos\left(\theta_{\mathrm{ou}} + 2\pi/3\right) \end{bmatrix} \cdot \frac{u_{\mathrm{dc}}}{\sqrt{3}} = T_{\mathrm{VSI}} \frac{u_{\mathrm{dc}}}{\sqrt{3}} \quad (3)$$

where T_{VSI} is the transfer function matrix of VSI and is called the modulation signals of VSI in this paper; θ_{ou} is the (reference) phase angle of output voltage vector; m_v is the voltage modulation index of VSI, defined as

$$m_{\mathrm{v}} = \sqrt{3} u_{\mathrm{om}}/u_{\mathrm{dc}} \quad (4)$$

where u_{om} is the output voltage amplitude; u_{dc} is the dc-link voltage. The modulation index of MC is the multiplication of m_c and m_v

$$m = m_{\mathrm{c}} m_{\mathrm{v}}. \quad (5)$$

Variables *m*, θ_{ii}, and θ_{ou} decide all the duty cycles of current vectors and voltage vectors in SVM of MC. So long as they maintain invariable, the actual input currents and output voltages of MC will not change.

Equation (1)–(5) show the mathematical model of MC modulated by SVM in the three-phase stationary frame [27]. Based

on these equations, the simplified model in two-phase stationary frame (i.e., $\alpha\beta$ frame) can be derived. First, (6) is got from (1)

$$\begin{bmatrix} i_{\mathrm{i}\alpha} \\ i_{\mathrm{i}\beta} \end{bmatrix} = m_{\mathrm{c}} \begin{bmatrix} \cos\theta_{\mathrm{ii}} \\ \sin\theta_{\mathrm{ii}} \end{bmatrix} i_{\mathrm{dc}} = \begin{bmatrix} m_{\mathrm{c}\alpha} \\ m_{\mathrm{c}\beta} \end{bmatrix} i_{\mathrm{dc}} \tag{6}$$

where $i_{i\alpha}$ and $i_{i\beta}$ are the $\alpha\beta$-axis input currents; $m_{c\alpha}$ and $m_{c\beta}$ are the $\alpha\beta$-axis modulation signals of CSR. Similarly, for VSI, (3) becomes (7) in $\alpha\beta$ frame

$$\begin{bmatrix} u_{\mathrm{o}\alpha} \\ u_{\mathrm{o}\beta} \end{bmatrix} = m_{\mathrm{v}} \begin{bmatrix} \cos\theta_{\mathrm{ou}} \\ \sin\theta_{\mathrm{ou}} \end{bmatrix} \frac{u_{\mathrm{dc}}}{\sqrt{3}} = \begin{bmatrix} m_{\mathrm{v}\alpha} \\ m_{\mathrm{v}\beta} \end{bmatrix} \frac{u_{\mathrm{dc}}}{\sqrt{3}} \tag{7}$$

where $u_{o\alpha}$ and $u_{o\beta}$ are the $\alpha\beta$-axis output voltages; $m_{v\alpha}$ and $m_{v\beta}$ are the $\alpha\beta$-axis modulation signals of VSI.

Since there is no energy storage element in MC, instantaneous active power at input side, dc-link side, and output side should be equal to each other, videlicet

$$p = 1.5\left(u_{\mathrm{i}\alpha}i_{\mathrm{i}\alpha} + u_{\mathrm{i}\beta}i_{\mathrm{i}\beta}\right) = u_{\mathrm{dc}}i_{\mathrm{dc}} = 1.5\left(u_{\mathrm{o}\alpha}i_{\mathrm{o}\alpha} + u_{\mathrm{o}\beta}i_{\mathrm{o}\beta}\right) \tag{8}$$

where *p* is the active power transferred by MC and is calculated based on the instantaneous power theory [28]; $u_{i\alpha}$ and $u_{i\beta}$ are the $\alpha\beta$-axis input voltages (i.e., capacitor voltages); $i_{o\alpha}$ and $i_{o\beta}$ are the $\alpha\beta$-axis output currents. By substitution (6) into (8), dc-link voltage u_{dc} is given by

$$u_{\mathrm{dc}} = 1.5(m_{\mathrm{c}\alpha}u_{\mathrm{i}\alpha} + m_{\mathrm{c}\beta}u_{\mathrm{i}\beta}). \tag{9}$$

The voltage drop across the filter inductor is negligible, hence

$$\begin{bmatrix} u_{\mathrm{i}\alpha} \\ u_{\mathrm{i}\beta} \end{bmatrix} \approx \begin{bmatrix} u_{\mathrm{s}\alpha} \\ u_{\mathrm{s}\beta} \end{bmatrix} = u_{\mathrm{sm}} \begin{bmatrix} \cos\theta_{\mathrm{su}} \\ \sin\theta_{\mathrm{su}} \end{bmatrix} \tag{10}$$

where $u_{s\alpha}$ and $u_{s\beta}$ are the $\alpha\beta$-axis source voltages; u_{sm} is the amplitude of source voltage; θ_{su} is the phase angle of source voltage vector. Then according to (6) and (10), (9) is simplified as

$$u_{\mathrm{dc}} \approx 1.5m_{\mathrm{c}}u_{\mathrm{sm}}\cos\Delta\theta_{\mathrm{is}}, \quad \Delta\theta_{\mathrm{is}} = \theta_{\mathrm{ii}} - \theta_{\mathrm{iu}} \tag{11}$$

where $\Delta\theta_{\mathrm{is}}$ is approximately the input power factor. Likewise, the dc-link current is obtained by substitution of (4) into (8)

$$i_{\mathrm{dc}} = \sqrt{3}m_{\mathrm{v}}(u_{\mathrm{o}\alpha}i_{\mathrm{o}\alpha} + u_{\mathrm{o}\beta}i_{\mathrm{o}\beta})/2u_{\mathrm{om}}. \tag{12}$$

The typical vector control of PMSM is often realized in two-phase rotating frame (i.e., *dq* frame). So the active power *p* at the output side shown in (8) and the dc-link current i_{dc} shown in (12) can also be calculated in *dq* frame, which is employed in experiments of this paper. Nevertheless, to keep consistent between the models of CSR and VSI, the analysis is given in $\alpha\beta$ frame. (6)–(12) represent the relationships among voltages, currents, and active power at input side, dc-link side, and output side, where modulation signals serve as the bond. The equations constructing the model of MC help to understand the traditional and new methods of modulation signals generation.

B. Methods of Modulation Signals Generation

In practice, the modulation signals of MC, i.e., *m*, θ_{ii}, and θ_{ou}, are generated from the voltages and currents at input and output side. It is a general assumption that, no matter how the generation is realized, the primary goal is to produce expected voltages at output side, which means the output voltage control must hold the highest priority. Various generation methods were proposed in previous works [27], [29], [30]. The principle of one typical and traditional method [27] is shown in Fig. 2(a), including four steps as follows.

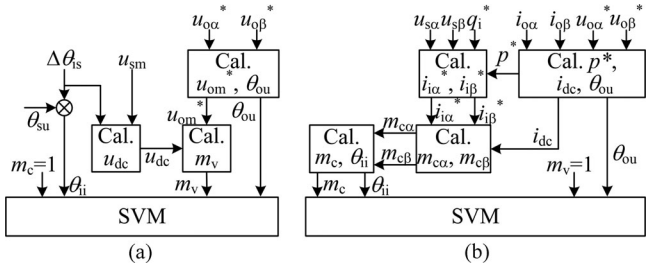

Fig. 2. Traditional and new methods to generate modulation signals (a) Traditional method (b) New method.

Step 1: Set m_c and $\Delta\theta_{\mathrm{is}}$. For maximizing voltage utilization ratio, m_c and $\Delta\theta_{\mathrm{is}}$ are normally set to 1 and 0 separately. As a result, the input current vector angle θ_{ii} is calculated by

$$\theta_{\mathrm{ii}} = \theta_{\mathrm{su}} + \Delta\theta_{\mathrm{is}}. \tag{13}$$

Step 2: Calculate the dc-link voltage u_{dc} with (14). It is based on (11) with $m_c = 1$

$$u_{\mathrm{dc}} \approx 1.5u_{\mathrm{sm}}\cos\Delta\theta_{\mathrm{is}}. \tag{14}$$

Step 3: Use $u^*_{o\alpha}$ and $u^*_{o\beta}$ to calculate the amplitude and phase angle of output voltage vector, i.e., u^*_{om} and θ_{ou}, based on coordinate transformation. The typical vector control of PMSM generates the reference values of $\alpha\beta$-axis output voltages, namely $u^*_{o\alpha}$ and $u^*_{o\beta}$.

Step 4: Calculate the modulation index m_v of VSI based on (4)

$$m_{\mathrm{v}} = \sqrt{3}u^*_{\mathrm{om}}/u_{\mathrm{dc}} = 2u^*_{\mathrm{om}}/\left(\sqrt{3}u_{\mathrm{sm}}\cos\Delta\theta_{\mathrm{is}}\right). \tag{15}$$

Then, the modulation index of MC is got by multiplication of m_c and m_v

$$m = m_{\mathrm{c}}m_{\mathrm{v}} = 2u^*_{\mathrm{om}}/\left(\sqrt{3}u_{\mathrm{sm}}\cos\Delta\theta_{\mathrm{is}}\right). \tag{16}$$

After *m*, θ_{ii}, and θ_{ou} are obtained, the SVM of MC can be implemented.

Although other generation methods, such as those in [29] and [30], do not fix m_c to one mandatorily or even let m_c variable, they share the same idea with [27], the dc-link voltage is first generated by the modulation of CSR and, then, is used to produce the expected output voltages through the modulation of VSI. In such methods, the output voltages are directly synthesized with input voltages, while the input currents are passively synthesized with output currents. From this point of view, the amplitude of input currents cannot be controlled directly [1], [2]. This leads to difficulties in realization of active damping control strategies through controlling input currents, for the reason that both the amplitude and phase angle of input currents are required to be directly controllable in such strategies.

In order to solve this problem, meanwhile ensuring the highest priority of output voltage control, an improvement of the traditional method is made by this paper, and the principle of it

is shown in Fig. 2(b). The new method consists of four steps as follows.

Step 1: Calculate $u^*_{\rm om}$ and $\theta_{\rm ou}$ using $u^*_{o\alpha}$ and $u^*_{o\beta}$. This step is the same as step 3 in traditional method.

Step 2: Set m_v to 1. Then, $i_{\rm dc}$ is got according to (12), and shown in (17)

$$i_{\rm dc} = \sqrt{3}(u^*_{\rm o\alpha} i_{o\alpha} + u^*_{\rm o\beta} i_{o\beta})/2u^*_{\rm om}. \tag{17}$$

Meanwhile, the required active power transferred by IMC is

$$p^* = 1.5(u^*_{\rm o\alpha} i_{o\alpha} + u^*_{\rm o\beta} i_{o\beta}). \tag{18}$$

Step 3: Set the reference value of input reactive power to q^*_i. With p^* obtained in step 2, the reference values of $\alpha\beta$-axis input currents can be calculated based on instantaneous power theory [28], and are expressed as

$$\begin{cases} i^*_{\rm i\alpha} = (p^* u_{\rm s\alpha} - q^*_{\rm i} u_{\rm s\beta})/1.5u^2_{\rm sm} \\ i^*_{\rm i\beta} = (p^* u_{\rm s\beta} + q^*_{\rm i} u_{\rm s\alpha})/1.5u^2_{\rm sm} \end{cases} \tag{19}$$

where q^*_i can be set in an open-loop way or in a closed-loop way. For example, q^*_i could come from the closed-loop control of source reactive power, so as to realize unit power factor operation at source side.

Step 4: Calculate $\alpha\beta$-axis modulation signals of CSR, according to (6) and (17)–(19)

$$\begin{cases} m_{\rm c\alpha} = i^*_{\rm i\alpha}/i_{\rm dc} = (p^* u_{\rm s\alpha} - q^*_{\rm i} u_{\rm s\beta})/(1.5u^2_{\rm sm} i_{\rm dc}) \\ m_{\rm c\beta} = i^*_{\rm i\beta}/i_{\rm dc} = (p^* u_{\rm s\beta} + q^*_{\rm i} u_{\rm s\alpha})/(1.5u^2_{\rm sm} i_{\rm dc}) \end{cases}. \tag{20}$$

Then, m_c and $\theta_{\rm ii}$ are calculated further as

$$m_{\rm c} = \sqrt{m^2_{\rm c\alpha} + m^2_{\rm c\beta}}, \theta_{\rm ii} = \text{atan2}(m_{c\beta}, m_{\rm c\alpha}) \tag{21}$$

where function atan2(y, x) is the arc tangent of the two variables x and y. In particular, if $\Delta\theta_{\rm is}$ is specified directly just as the traditional method, the input reactive power can be expressed as $q_i = p^* tan\Delta\theta_{is}$. So with the substitution of (17) and (18), (20) and (21) can be simplified as (22) and (23), respectively,

$$\begin{cases} m_{\rm c\alpha} = 2u^*_{\rm om}(u_{\rm s\alpha} - u_{\rm s\beta}\tan\Delta\theta_{\rm is})/\sqrt{3}u^2_{\rm sm} \\ m_{\rm c\beta} = 2u^*_{\rm om}(u_{\rm s\beta} + u_{\rm s\alpha}\tan\Delta\theta_{\rm is})/\sqrt{3}u^2_{\rm sm} \end{cases} \tag{22}$$

$$m_{\rm c} = 2u^*_{\rm om}/\left(\sqrt{3}u_{\rm sm}\cos\Delta\theta^*_{\rm is}\right), \quad \theta_{\rm ii} = \theta_{\rm su} + \Delta\theta_{\rm is}. \tag{23}$$

Then, the modulation index of MC is got

$$m = m_{\rm c} m_{\rm v} = 2u_{\rm om}/\left(\sqrt{3}u_{\rm sm}\cos\Delta\theta_{\rm is}\right) \tag{24}$$

which is the same with that in traditional method, so is $\theta_{\rm ii}$ and $\theta_{\rm ou}$. Therefore, if the new method and traditional method both specifies the value of $\Delta\theta_{\rm is}$, the same input currents and output voltages will be obtained. In this way, they are equivalent from an input–output point of view.

From the steps described above and Fig. 2, we can find the basic idea of the new method. Different from the traditional method, the new method first generates the dc-link current by the modulation and VSI and, then, employs it to produce the expected input currents through the modulation of CSR. Hence, the input currents are directly synthesized with output currents, while the output voltages are indirectly synthesized with input voltages. However, the reference values of input currents are dependent on the expected output active power. From the viewpoint of system control, the output voltage control is the outer loop, while the input current control is the inner. Consequently, it ensures the top priority of output voltage control. So the new method provides a feasible way to directly control the amplitude and phase angle of input currents without affecting the output voltage control.

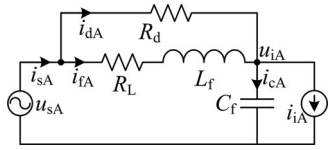

Fig. 3. *LC* filter circuit with passive damping control.

By using the new method to generate modulation signals, it is very easy to realize some control strategies, which require directly controllable amplitude and phase angle of input currents and preferential output voltage control. For example, the closed-loop control of source currents can be achieved without any interfere with closed-loop control of output current existing in the method presented by [22]. Based on the new method, this paper realizes an active damping control strategy via modifying input reference currents.

III. Active Damping Control Strategy via Modifying Input Reference Currents

A. Spectrum of the LC Filter With Passive Damping Resistor

The phase A circuit of *LC* filter with typical passive damping control [14] is illustrated in Fig. 3. A passive damping resistor R_d is paralleled with filter inductor L_f. L_f is serialized with its resistance R_L, which is small and negligible. Noninductive filter capacitor C_f is considered ideal. The parameters of filter in this paper are: $L_f = 1$ mH, $R_L = 0.3\ \Omega$, $C_f = 12.6\ \mu$F. From Fig. 3, we can get the circuit equations of phase A

$$\begin{cases} L_{\rm f}\dfrac{{\rm d}i_{\rm fA}}{{\rm d}t} = u_{\rm sA} - u_{\rm iA} - R_{\rm L} i_{\rm fA} \\ C_{\rm f}\dfrac{{\rm d}u_{\rm iA}}{{\rm d}t} = i_{\rm fA} + i_{\rm dA} - i_{\rm iA} \\ i_{\rm dA} = (u_{\rm sA} - u_{\rm iA})/R_{\rm d} \\ i_{\rm sA} = i_{\rm fA} + i_{\rm dA} \end{cases} \tag{25}$$

where u_{sA} is the source voltage; i_{sA} is the source current; u_{iA} is the input voltage of MC, namely the capacitor voltage; i_{fA} is the inductor current; i_{dA} is the current flowing through damping resistor. In the source voltage vector oriented *dq* frame, the *d*-axis and *q*-axis currents represent the active and reactive currents, respectively. To analyze the effects of the *LC* filter on source currents when load changes, (25) is transformed to the *dq* frame, resulting in the state-space equation of the *LC* filter shown in (26)

$$\begin{cases} \dfrac{{\rm d}x}{{\rm d}t} = Ax + Bu \\ y = Cx + Du \end{cases} \tag{26}$$

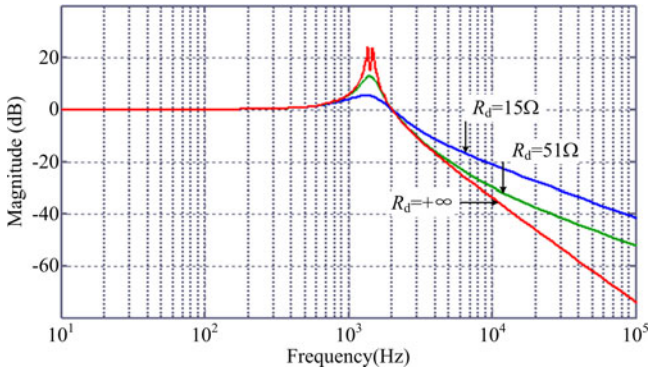

Fig. 4. Spectrum of transfer function from i_{id} to i_{sd} in passive damping control.

where state variable x is $[i_{fd}, i_{fq}, u_{id}, u_{iq}]^{\mathrm{T}}$ ($[\cdot]^{\mathrm{T}}$ represents the matrix transposition of $[\cdot]$); input variable u is $[u_{sd}, u_{sq}, i_{id}, i_{iq}]^{\mathrm{T}}$; output variable y is $[i_{sd}, i_{sq}]^{\mathrm{T}}$. The matrices in (28) are expressed as follows:

$$A = \begin{bmatrix} -R_L/L_f & \omega_s & -1/L_f & 0 \\ -\omega_s & -R_L/L_f & 0 & -1/L_f \\ 1/C_f & 0 & -1/R_dC_f & \omega_s \\ 0 & 1/C_f & -\omega_s & -1/R_dC_f \end{bmatrix}$$

$$B = \begin{bmatrix} 1/L_f & 0 & 0 & 0 \\ 0 & 1/L_f & 0 & 0 \\ 1/R_dC_f & 0 & -1/C_f & 0 \\ 0 & 1/R_dC_f & 0 & -1/C_f \end{bmatrix}$$

$$C = \begin{bmatrix} 1 & 0 & -1/R_d & 0 \\ 0 & 1 & 0 & -1/R_d \end{bmatrix} D = \begin{bmatrix} 1/R_d & 0 & 0 & 0 \\ 0 & 1/R_d & 0 & 0 \end{bmatrix}$$

where ω_s is the angular frequency of source voltage. The spectrum of the transfer function from i_{id} to i_{sd} with different R_d is illustrated in Fig. 4. From Fig. 4, it can be observed that smaller R_d results in smaller magnitude at resonant frequency, but larger magnitude at high frequency. Therefore, increasing damping performance of passive damping control will lead to the decrease of filtering performance.

The dual characters of R_d lie in that, high-frequency current flows through it when damping oscillations, which is also a part of source current. Hence, reducing the value of R_d will inevitably increase higher harmonics in source current.

B. Principle of the Proposed Active Damping Control Strategy

Supposing R_d is not installed in Fig. 3, equivalently $R_d = +\infty$, then from Fig. 4, we know that the damping coefficient is very small and the oscillations are likely to be excited by harmonic currents. To suppress the oscillations as in passive damping control, the proposed active damping control strategy is applied to the filter, of which the equivalent circuit is depicted in Fig. 5. In Fig. 5, R_{vd} is the virtual damping resistor; i_{iAe} is the additional damping signal and $i_{iA'}$ is the input current injected with i_{iAe}.

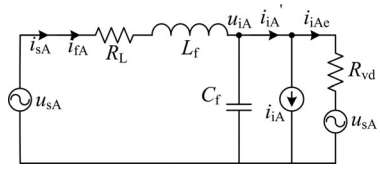

Fig. 5. Equivalent circuit of *LC* filter with the proposed active damping control.

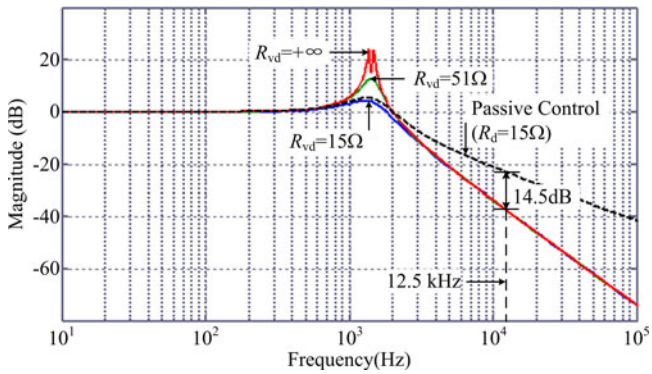

Fig. 6. Spectrum of transfer function from i_{id} to i_{sd} in active damping control.

Still take the same variables in passive damping control to establish the new state-space equation. According to Fig. 5, the new matrices are

$$A = \begin{bmatrix} -R_L/L_f & \omega_s & -1/L_f & 0 \\ -\omega_s & -R_L/L_f & 0 & -1/L_f \\ 1/C_f & 0 & -1/R_{\mathrm{vd}}C_f & \omega_s \\ 0 & 1/C_f & -\omega_s & -1/R_{\mathrm{vd}}C_f \end{bmatrix}$$

$$B = \begin{bmatrix} 1/L_f & 0 & 0 & 0 \\ 0 & 1/L_f & 0 & 0 \\ 1/R_{\mathrm{vd}}C_f & 0 & -1/C_f & 0 \\ 0 & 1/R_{\mathrm{vd}}C_f & 0 & -1/C_f \end{bmatrix}$$

$$C = \begin{bmatrix} 1 & 0 & 0 & 0 \\ 0 & 1 & 0 & 0 \end{bmatrix} D = \begin{bmatrix} 0 & 0 & 0 & 0 \\ 0 & 0 & 0 & 0 \end{bmatrix}.$$

It is obvious that, system matrix A in the proposed strategy has the same form with that in passive damping control. As matrix A contains the damping information of *LC* filter, the proposed strategy can also increase the damping coefficient. Fig. 6 illustrates the spectrum of transfer function from i_{id} to i_{sd} in active damping control. From Fig. 6, we can know that smaller R_{vd} results in lower magnitude at resonant frequency, but doesn't change the magnitude at high frequency. This means that the proposed strategy can achieve good damping performance and filtering performance at the same time.

The spectrum of transfer function in passive damping control with $R_d = 15\,\Omega$ is also shown in Fig. 6. The steady-state equations and the spectrum of the *LC* filter in passive damping control are compared with those in active damping control. It can be drawn from the comparison that since in passive damping control R_d exists in matrix *C*, while in active damping control $R_{\rm vd}$ does not appears in matrix *C*, the transfer function of the *LC* filter in passive damping control has one more zero than that in active damping control. This brings about the following two aspects for consideration.

1) Zeros could decrease the damping coefficient. Hence, the active damping control provides larger damping coefficient than passive damping control with $R_d = R_{\rm vd}$. However, when the parameters of the *LC* filter and damping resistors are selected appropriately, the damping coefficient is mainly decided by matrix *A*. Therefore, it is certain that the two methods have the same damping performance. Besides, if the proposed strategy is completely realized, the adjusting ranges of the physical resistor and virtual damping resistor are logically the same in the two methods.
2) Zeros have high impact on the filtering performance. As it can be seen from Figs. 4 and 6, the gain at high frequency in the active damping control is smaller than that in passive damping control. The differences become more obvious with the reduction of passive damping resistor and the increase of frequency. In particular, when $R_d = R_{\rm vd} = 15\,\Omega$, the difference at 12.5 kHz (the switching frequency of CSR in experiments) is 14.5 dB, which means that the harmonics of source currents around 12.5 kHz in passive damping control are about 5.3 times of that in active damping control. Hence, the proposed strategy can reduce the high frequency harmonics significantly.

In conclusion, the proposed active damping control strategy has the same damping performance with passive damping control, but better filtering performance, when completely realized.

C. Realization of the Proposed Strategy

To completely realize the proposed strategy depicted in Fig. 5, the new method of modulation signals generation should be applied with just modifying the input reference currents $i_{i\alpha}^*$ and $i_{i\beta}^*$ as

$$\begin{cases} i_{\rm i\alpha}^{**} = i_{\rm i\alpha}^* + i_{\rm i\alpha e} \\ i_{\rm i\beta}^{**} = i_{\rm i\beta}^* + i_{\rm i\beta e} \end{cases} \tag{27}$$

where $i_{i\alpha e}$ and $i_{i\beta e}$ are additional $\alpha\beta$-axis damping signals and have the expressions of

$$\begin{cases} i_{\rm i\alpha e} = (u_{\rm i\alpha} - u_{\rm s\alpha})/R_{\rm vd} \\ i_{\rm i\beta e} = (u_{\rm i\beta} - u_{\rm s\beta})/R_{\rm vd} \end{cases} \tag{28}$$

which means the damping signals are proportional to the voltage drop across the filter inductor. Measuring capacitor voltages to calculate $i_{i\alpha e}$ and $i_{i\beta e}$ is an effective way. Alternatively, $\alpha\beta$-axis source currents, i.e., $i_{s\alpha}$ and $i_{s\beta}$, can also be used to construct

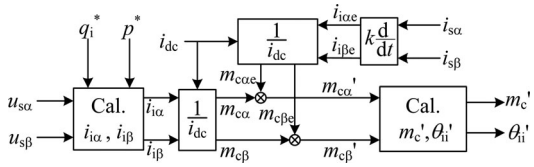

Fig. 7. Calculation of modified input currents and modulation signals.

(28), as shown in (29)

$$\begin{cases} i_{\rm i\alpha e} = -\dfrac{1}{R_{\rm vd}}\left(L_{\rm f}\dfrac{{\rm d}i_{\rm s\alpha}}{{\rm d}t} + R_{\rm L}i_{\rm s\alpha}\right) \\ i_{\rm i\beta e} = -\dfrac{1}{R_{\rm vd}}\left(L_{\rm f}\dfrac{{\rm d}i_{\rm s\beta}}{{\rm d}t} + R_{\rm L}i_{\rm s\beta}\right) \end{cases}. \tag{29}$$

Theoretically, (29) is completely equivalent with (28). The source currents contain few high-frequency harmonics when the physical damping resistor is not installed [3]. Therefore, the derivation operation in (29) is achievable in practice.

With modified reference value of input currents obtained in (27), the modified $\alpha\beta$-axis modulation signals of CSR, namely $m_{c\beta}'$ and $m_{c\beta}'$, can be calculated, as shown in Fig. 7. According to (6), the expressions of $m_{c\alpha}'$ and $m_{c\beta}'$ are

$$\begin{cases} m_{\rm c\alpha}' = i_{\rm i\alpha}^{**}/i_{\rm dc} \\ m_{\rm c\beta}' = i_{\rm i\beta}^{**}/i_{\rm dc} \end{cases}. \tag{30}$$

Based on (27), rewriting (30) as

$$\begin{cases} m_{\rm c\alpha}' = m_{\rm c\alpha} + m_{\rm c\alpha e} \\ m_{\rm c\beta}' = m_{\rm c\beta} + m_{\rm c\beta e} \end{cases} \tag{31}$$

where $m_{c\alpha}$ and $m_{c\beta}$ are the modulation signals without modification shown in (20) or (22), of which the function is to adjust the amplitude of output voltage; $m_{c\alpha e}$ and $m_{c\beta e}$ are additional damping signals in modulation signals and are used to suppress oscillations in source currents. The expressions of $m_{c\alpha e}$ and $m_{c\beta e}$ are

$$\begin{cases} m_{\rm c\alpha e} = i_{\rm i\alpha e}/i_{\rm dc} \\ m_{\rm c\beta e} = i_{\rm i\beta e}/i_{\rm dc} \end{cases}. \tag{32}$$

Appropriate values of the filter inductor bring about small voltage drop [14]. Hence, $i_{i\alpha e}$ and $i_{i\beta e}$ are only a very small proportion of $i_{i\alpha}^{**}$ and $i_{i\beta}^{**}$, which is also true for $m_{c\alpha e}$ and $m_{c\beta e}$ in $m_{c\alpha}'$ and $m_{c\beta}'$. Particularly, the fundamental frequency components in $i_{i\alpha e}$ and $i_{i\beta e}$ are almost 0. So the proposed active damping control strategy has little influence on normal operation of MC. Besides, this also proves that the control range of input currents in the proposed strategy is the same with that in passive damping control, without any special limitation.

After m_c' and $\theta_{\rm ii}'$ of CSR are calculated by using $m_{c\alpha}'$ and $m_{c\beta}'$, SVM of MC can be implemented through combining them with the modulation signals of VSI, i.e., $m_v = 1$ and $\theta_{\rm ou}$.

It is important to note that, the operation mode of MC is not the precondition when applying the proposed strategy. Actually, the operation mode is reflected by the sign of $i_{\rm dc}$ and, thus, is contained in the calculation of the additional damping modulation signals in (32). Therefore, the proposed strategy is effective

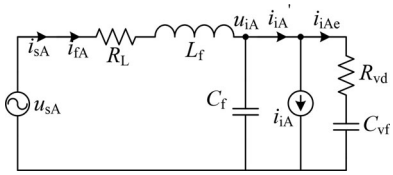

Fig. 8. Equivalent circuit of *LC* filter with another active damping control.

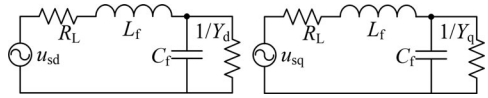

Fig. 9. *Dq*-axis small-signal model of the *LC* filter.

no matter MC works in motoring mode or generating mode. This is naturally true because the equivalent circuit shown in Fig. 5 is completely realized, which are the same in both modes.

D. Realization of the Previous Method

The idea of emulating physical damping resistors to realize active damping control is not new. A similar method has been proposed and applied in previous works [20], [21], [23], [31], [32], of which the principle is shown in Fig. 8. In this method, a virtual branch consisting of a resistor and capacitor in series is paralleled to the physical filtering capacitors. Some existing works try to realize such a method. Rivera *et al.* [20], [21] realized it by controlling output currents, while [31], [32] by digitally filtering the amplitude of capacitor voltages in modulation, which are only approximate methods. Sato *et al.* [23] realized it by simply modifying the modulation signals under the condition that input currents are independently controllable, which is strictly limited as stated in introduction.

Nevertheless, the new method of modulation signals generation presented in Section II, makes it very convenient to completely realize this active damping method, without requiring independent controllable input currents. To achieve this goal, the additional damping signals shown in (33) are injected into input reference currents. Then the procedure in part C of this section can be used to realize this

$$\begin{cases} i_{\mathrm{i}\alpha\mathrm{e}} = \dfrac{sC_{\mathrm{vf}}}{sR_{\mathrm{vd}}C_{\mathrm{vf}}+1}u_{\mathrm{i}\alpha} \\ i_{\mathrm{i}\beta\mathrm{e}} = \dfrac{sC_{\mathrm{vf}}}{sR_{\mathrm{vd}}C_{\mathrm{vf}}+1}u_{\mathrm{i}\beta} \end{cases}. \tag{33}$$

Rewrite (33) as

$$\begin{cases} i_{\mathrm{i}\alpha\mathrm{e}} = K_{\mathrm{d}}\dfrac{sT_{\mathrm{d}}}{sT_{\mathrm{d}}+1}u_{\mathrm{i}\alpha} \\ i_{\mathrm{i}\beta\mathrm{e}} = K_{\mathrm{d}}\dfrac{sT_{\mathrm{d}}}{sT_{\mathrm{d}}+1}u_{\mathrm{i}\beta} \end{cases}, \quad K_{\mathrm{d}} = \frac{1}{R_{\mathrm{vd}}}, \quad T_{\mathrm{d}} = R_{\mathrm{vd}}C_{\mathrm{vf}}. \tag{34}$$

(34) means that the damping signals can be calculated with capacitor voltages filtered by high-pass digital filters, where K_d is the proportional coefficient and T_d is the time constant. Similar to those in [16]–[21], [23], [31], and [32], $i_{i\alpha e}$ and $i_{i\beta e}$ in (34) provide larger damping coefficient when K_d and T_d increase. At the same time, (34) shows that the additional damping signals contain fundamental frequency components, which would impact the normal operation of MC. With the increase of K_d and T_d, the impact cannot be neglected. As a result, the damping performance of this method is limited. Such problem doesn't exist in the proposed strategy shown in Fig. 5, which would be the better solution from the viewpoint of damping performance. But the method shown in Fig. 8 has the advantage that it does not need any extra voltage or current sensor if capacitor voltages are sampled for modulation. Therefore, combing this method with typical passive damping control is more meaningful, just as what [21], [23] have done.

IV. Discussion About the Proposed Active Damping Control Strategy

A. Applicability to the Case With Capacitor Voltages Sampled for Modulation

In Sections II and III, the proposed strategy uses source voltages for modulating MC. However, in the situation of generator input where source voltages cannot be sampled, the capacitor voltages are needed in order to generate modulation signals. Most of existing active damping methods are aimed at this case [16]–[19], [22], [23], [31], [32]. By replacing source voltages with capacitor voltages in (19), the input reference currents without modification are got. With the substitution of them and the additional damping signals shown in (28) into (27), the modified $\alpha\beta$-axis reference values of input currents in this case can be expressed as

$$\begin{cases} i_{\mathrm{i}\alpha}^{**} = \dfrac{2p^*u_{\mathrm{i}\alpha}}{3u_{\mathrm{im}}^2} - \dfrac{2q_{\mathrm{i}}^*u_{\mathrm{i}\beta}}{3u_{\mathrm{im}}^2} + \dfrac{u_{\mathrm{i}\alpha}-u_{\mathrm{s}\alpha}}{R_{\mathrm{vd}}} \\ i_{\mathrm{i}\beta}^{**} = \dfrac{2p^*u_{\mathrm{i}\beta}}{3u_{\mathrm{im}}^2} + \dfrac{2q_{\mathrm{i}}^*u_{\mathrm{i}\alpha}}{3u_{\mathrm{im}}^2} + \dfrac{u_{\mathrm{i}\beta}-u_{\mathrm{s}\beta}}{R_{\mathrm{vd}}} \end{cases} \tag{35}$$

where u_{im} is the amplitude of capacitor voltage, the additional damping signals should be calculated by (29) instead of (28) in practice, for the source voltages are unavailable. Transforming (35) into *dq* frame, we can get the modified *dq*-axis input currents

$$\begin{cases} i_{\mathrm{id}}^{**} = \dfrac{2p^*u_{\mathrm{id}}}{3u_{\mathrm{im}}^2} - \dfrac{2q_{\mathrm{i}}^*u_{\mathrm{iq}}}{3u_{\mathrm{im}}^2} + \dfrac{u_{\mathrm{id}}-u_{\mathrm{sd}}}{R_{\mathrm{vd}}} \\ i_{\mathrm{iq}}^{**} = \dfrac{2p^*u_{\mathrm{iq}}}{3u_{\mathrm{im}}^2} + \dfrac{2q_{\mathrm{i}}^*u_{\mathrm{id}}}{3u_{\mathrm{im}}^2} + \dfrac{u_{\mathrm{iq}}-u_{\mathrm{sq}}}{R_{\mathrm{vd}}} \end{cases} \tag{36}$$

where u_{id} and u_{iq} are *dq*-axis capacitor voltages; u_{sd} and u_{sq} are *dq*-axis source voltages. The circuit equations of the filter are nonlinear as the input currents are nonlinearly correlative to the state variables. So the *dq*-axis small-signal model shown in Fig. 9 is used to analyze the system stability [16], [33], where the *dq*-axis input admittances y_d and y_q are

$$\begin{cases} y_{\mathrm{d}} = \partial i_{\mathrm{id}}/\partial u_{\mathrm{id}} \\ y_{\mathrm{q}} = \partial i_{\mathrm{iq}}/\partial u_{\mathrm{iq}} \end{cases}. \tag{37}$$

At steady-state operation point, the expressions of them are

$$\begin{cases} Y_{\rm d} = \dfrac{2P(U_{\rm iq}^2 - U_{\rm id}^2)}{3U_{\rm im}^4} - \dfrac{4Q_{\rm i}U_{\rm id}U_{\rm iq}}{3U_{\rm im}^4} + \dfrac{1}{R_{\rm vd}} \\ Y_{\rm q} = \dfrac{2P(U_{\rm id}^2 - U_{\rm iq}^2)}{3U_{\rm im}^4} - \dfrac{4Q_{\rm i}U_{\rm id}U_{\rm iq}}{3U_{\rm im}^4} + \dfrac{1}{R_{\rm vd}} \end{cases} \tag{38}$$

where P, Q_i, U_{id}, U_{iq}, and $U_{\rm im}$ are the corresponding steady values. Since U_{iq} is much smaller than $U_{\rm im}$, the items containing U_{iq} in (38) are ignorable. Then, we get that if $R_{\rm vd}$ satisfies

$$R_{\rm vd} < 1.5U_{\rm im}^2 / |P| \tag{39}$$

positive *dq*-axis input admittances are guaranteed in both motoring mode ($P > 0$) and generating mode ($P < 0$); thus, the system is small-signal stable [16], [33]. (39) also shows the the maximum value of the virtual resistor for the sake of system stability, which is also true for passive damping control.

The connotation of $R_{\rm vd}$ in (36) is the same with that in the case where source voltages are sampled for modulation. Hence, reducing $R_{\rm vd}$ could increase the damping coefficient and obtain good damping performance in steady state and dynamic process. It indicates that the proposed strategy can achieve the same damping performance with passive damping control and better filtering performance in this case, which are also insensitive to the operation mode of MC.

B. Realization Based on Other Modulation Algorithms

The modulation algorithms of MC are reviewed in [4], which include the four most intensively researched algorithms, namely Venturini algorithm, scalar algorithm, carrier-based algorithm, and space vector algorithm. As it is shown in Section II, the basic idea of the new method generation is using output currents to directly synthesize input currents, while generating the input reference currents with the expected output active power. If such an idea is applied to the above algorithms, the input currents can be directly controlled without affecting the priority of output voltage control and, thus, the proposed strategy can be realized completely.

For convenience, the extensions of the proposed strategy to other algorithms are provided here in detail. For most of the algorithms, $u_{\rm sm}$, $\theta_{\rm ii}$, $u_{\rm om}^*$, and $\theta_{\rm ou}$ are sufficient to modulate MC. According to (6) and (27), the modified $\theta_{\rm ii}$ are

$$\theta'_{\rm ii} = \operatorname{atan2}\left[\frac{i_{\rm i\beta}^* + i_{\rm i\beta e}}{i_{\rm dc}}, \quad \frac{i_{\rm i\alpha}^* + i_{\rm i\alpha e}}{i_{\rm dc}}\right] \tag{40}$$

where $i_{i\alpha}^*$ and $i_{i\beta}^*$ are calculated with (19); $i_{i\alpha e}$ and $i_{i\beta e}$ are calculated using (28) or (29); $i_{\rm dc}$ should be obtained using (17) (or its equivalent form in *dq*-frame) and it reflects the power flow direction in (40). As m_v is set to 1, the modified reference value of output voltage amplitude can easily be obtained by substitution of (31) and (9) into (4)

$$u_{\rm om}^{**} = \frac{u_{\rm dc}}{\sqrt{3}} = u_{\rm om}^* + \frac{\sqrt{3}}{2i_{\rm dc}}(u_{\rm s\alpha}i_{\rm i\alpha e} + u_{\rm s\beta}i_{\rm i\beta e}). \tag{41}$$

The source voltages used in the calculation of (40) and (41) can be replaced by capacitor voltages. It can be noticed that the final expressions of $\theta'_{\rm ii}$ in (40) and $u_{\rm om}^{**}$ in (41) just involve the voltages and currents at input and output side, which are independent of SVM, so is the case with $i_{\rm dc}$ in (17). Therefore, applying $\theta'_{\rm ii}$, $u_{\rm om}^{**}$ as well as the unchanged $u_{\rm sm}$ and $\theta_{\rm ou}$ to the above four modulation algorithms, the proposed active damping control strategy are realized completely. It proves that the proposed strategy is not restricted to SVM and can be extended to most of existing modulation algorithms. In particular, if (40) and (41) are applied simultaneously to the traditional method of generating SVM signals, the proposed strategy can also be realized. However, (40) and (41) are not easy to be derived based on the traditional method and have not been revealed by previous works.

The predictive current/torque control strategy and direct torque control strategy are also reviewed in [4], which belong to system control strategies. As the output currents are directly controlled in these strategies, the output reference voltages are not necessary. Hence, the proposed strategy cannot be applied to these strategies and further research should be done on this.

C. Comparison With Existing Methods

As stated above, most of existing active damping strategies focus on the small-signal stability [16]–[23], [31], [32]. Digital filters are very important in these strategies. For example, dc blockers are stilled applied to filter the capacitor voltages in [20], [21] even when the source voltages and source currents are also available. The digital filters worsen the dynamic performance [16], and even could limit the range of parameters adjustment [20], [21]. Hence, to a large extent, most of existing methods cannot match the typical passive damping control in the respect of damping performance. But the proposed strategy in this paper has the same damping performance and parameters range with passive damping control regardless of the operation mode of MC, no matter the source voltages or capacitor voltages are sampled for modulation. This is a major advantage of the proposed strategy over existing methods.

The method proposed by [16] has been the most comprehensive one so far. It can improve the small-signal stability effectively, which is realized by modifying the *d*-axis or *q*-axis reference values of output voltages when MC works in motoring mode, and modifying the phase angle of input current vector when MC works in generating mode. It can be seen from (40) and (41), the proposed strategy can also be viewed as a method realized by modifying the reference value of output voltage amplitude and phase angle of the input current vector. This may cause confusion with the general constructive method in [16]. However, as the proposed strategy is expected to obtain the same damping performance with passive damping control no matter source voltages or capacitor voltages are sampled for modulation, but not just aimed at the small signal stability, its principle is hardly to be directly explained by the method in [16]. What's more, there is a significant difference between the proposed strategy and the method in [16]. The general constructive method in motoring mode conflicts with that in generating mode as proved by [16], while the proposed strategy is suitable for both modes. Actually, (40) and (41) must be applied to the modulation of MC simultaneously in both modes, in order to obtain the required damping performance.

TABLE I
EXPERIMENTAL PARAMETERS

Variables	Description	Values
Source		
U_s	RMS Source Phase Voltage	155 (V)
f_s	Source Frequency	50 (Hz)
Source Side Filter		
L_f	Filter Inductor	1 mH
C_f	Filter Capacitor	12.6 μF
R_L	Resistance of Filter Inductor	0.3 Ω
IMC Power Setup		
IGBT	Power Module of CSR	APTGT50TDU60PG
Module	Power Module of VSI	PM 75RLA060
DSP	Digital Signal Processor	TMS 320F28335
CPLD	Complex Programmable Logic Device	EPM 1270T144C8N
ADC	Analog-to-Digital Converter	ADS 8568
DAC	Digital-to-Analog Converter	AD 5438
PMSM		
P_N	Rated Power	2.4 kW
n_N	Rated Speed	3000 r/min
f_{oN}	Rated Frequency of Stator Current	200 Hz
I_{oN}	RMS Rated Stator Current	9 A
U_{oN}	RMS Rated Stator Voltage	97 V
L_s	Stator Armature Inductance	1.23 mH
J	Moment of Inertia	$*$0.025 kg.m^2
Control Method (SVM-Based)		
f_{sampling}	Sampling Frequency	25 kHz
$f_{\mathrm{switching}}$	Switching Frequency of CSR	12.5 kHz
	Switching Frequency of VSI	25 kHz
R_d	Physical Damping Resistor	15 Ω
R_{vd}	Virtual Damping Resistor	15 Ω

$*$It is the sum of the moment of inertia of PMSM and the coaxial generator

One of the drawbacks of the proposed strategy is that it needs extra voltage or current sensors, which is the cost of the same damping performance as passive damping control. Besides, the minimum absolute value of i_{dc} in (32) should be limited, to prevent $m_{c\alpha e}$ and $m_{c\beta e}$ from getting too large due to the division operation. It usually takes place when the operation mode of MC switches from motoring mode to generating mode or reversely. The limit value is mainly dependent on the output currents ripple and sampling precision. As the limited interval in dynamic process is usually very short, such limitation has little effect on the damping performance. Hence it is still safe to say that the proposed strategy can obtain the same damping performance with passive damping control.

V. EXPERIMENTAL VERIFICATION

A. Experimental Prototype

In order to verify the effectiveness of the proposed active damping control strategy, this paper builds up a 2.4- kW IMC-fed PMSM drive prototype, of which the key parameters are shown in Table I. PMSM is coaxially connected with a synchronous generator, of which the load is pure resistors. The parameters of the *LC* filter are the same with that in Section III. The SVM of symmetrical switching pattern [2] is applied to IMC, resulting in different switching frequencies of CSR and VSI, which are 12.5 and 25 kHz separately.

On the built prototype, passive damping control and the proposed active damping control strategy are both experimentally verified and their performances in steady-state and dynamic process are compared accordingly. The resonant frequency of the *LC* filter is about 1.4 kHz. In passive damping control, a 15 Ω physical resistor is paralleled with the filter inductor. In active damping control, the physical resistor is removed and a virtual resistor of 15 Ω is applied in control algorithm, bringing about better filtering performance and the same damping performance. In both control strategies, the method to generate modulation signals is the new one presented in Section II, the control method of PMSM is the typical $i_d^* = 0$ vector control realized in *dq* frame, and the active power *p* and dc-link current i_{dc} are calculated in *dq* frame.

TABLE II
MAJOR PERFORMANCE OF SOURCE CURRENT, STATOR CURRENT, AND SPEED IN EXPERIMENTS

Items	Passive Damping	Active Damping
Source current at Rated Speed and Rated Power		
THD	4.13%	2.63%
Maximum Harmonic Content Around 1.4 kHz	1.19%	1.19%
Maximum Harmonic Content Around 12.5 kHz	1.62%	0.44%
Stator current at Rated Speed and Rated Power		
THD	7.34%	7.30%
Speed in Dynamic Process		
Rising/Falling Time	1.35s	1.35s
Overshoot	2.10%	2.10%

B. Experimental Results

The experimental results are illustrated in Figs. 10–14. The key performance of source currents, stator currents, and speed is shown in Table II. Detailed discussions about the experimental results are as follows.

Fig. 10 shows the stator current of PMSM and source current at rated speed and rated power, which are measured by current probes of 30- MHz wideband. From the figure, we can find that there is no difference between the two control methods in the waveform quality of stator currents. The total harmonic distortion (THD) in both methods is about 7.3%, as shown in Table II. THD of stator current is a little large due to the small armature inductance (just 1.23 mH) and relative high current frequency (200 Hz). Anyway, it can be concluded that the waveform quality of stator current in both methods is the same.

There are distinct differences between the waveform quality of source currents in the two methods. The waveform in passive damping control is thicker, reflecting larger high frequency harmonic contents. The spectral analysis results are shown in Fig. 11, which are completed in MATLAB with data provided by the current probes. The harmonic analysis results are shown in Table II. As can be seen from Fig. 11, harmonics mainly distribute below 3 kHz and around 12.5 kHz. The harmonics below 3 kHz come from the large ripple of stator currents and the nonlinearities of IMC in practice, such as the dead-time commutation, while the harmonics around 12.5 kHz are generated by the PWM control. In both methods, the harmonics below 3 kHz are approximately the same. In particular, the maximum harmonic content around 1.4 kHz (the resonant frequency of *LC* filter) is 1.19% in both modes as shown in Table II, demonstrating the same damping performance. However, the maximum harmonic

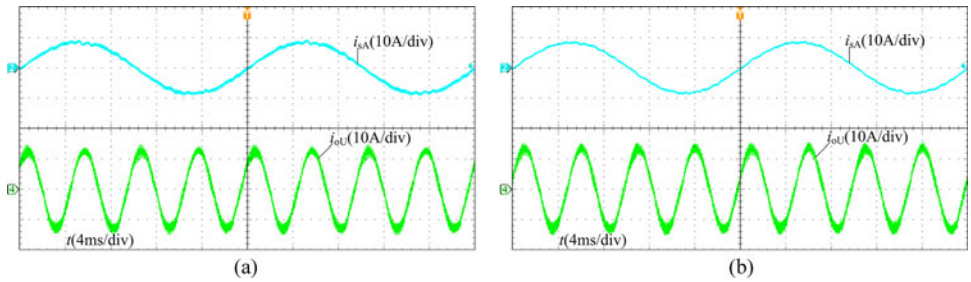

Fig. 10. Stator current (i_{oU}) of PMSM and source current (i_{sA}) at rated speed and rated power (a) Passive damping control. (b) Active damping control .

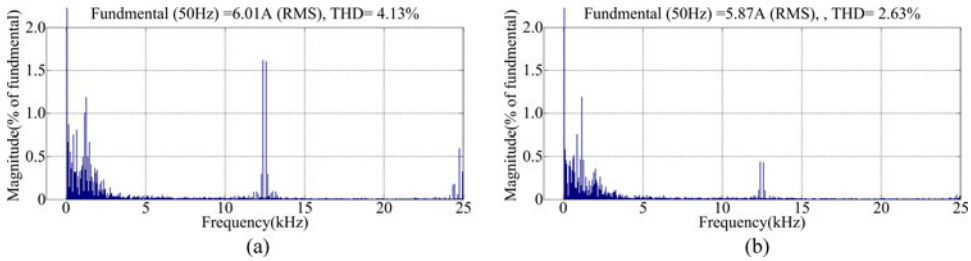

Fig. 11. Spectral analysis results of source current at rated speed and rated power (a) Passive damping control. (b) Active damping control.

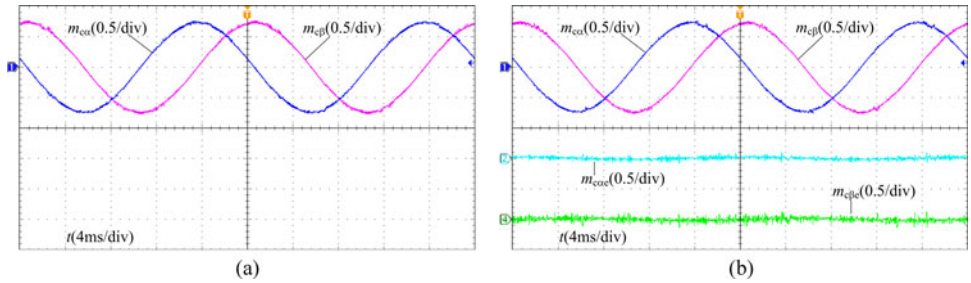

Fig. 12. Unmodified modulation signals ($m_{c\alpha}$ and $m_{c\beta}$) and the additional damping signals ($m_{c\alpha e}$ and $m_{c\beta e}$) at rated speed and rated power (a) Passive damping control. (b) Active damping control.

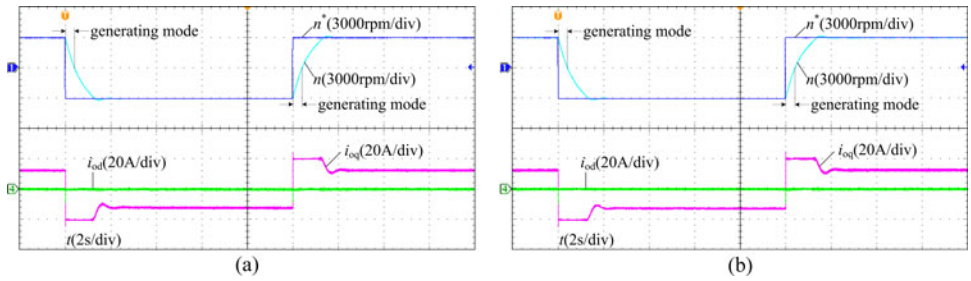

Fig. 13. Speed (n), d-axis (i_{od}), and q-axis (i_{oq}) currents of PMSM when speed reference (n^*) steps between 3000 and -3000 r/min (a) Passive damping control. (b) Active damping control.

content around the switching frequency in active damping control is significantly smaller than that in passive damping control, which is the main reason for the decreased THD in active damping control. The difference is about 3.7 times, which is smaller than the theoretical value presented in Section III. Even so, it can still prove that the proposed strategy has better filtering performance than passive damping control, considering the uncertainty of measurements. Besides, the RMS source current in active damping control is smaller, indicating that the proposed strategy improves the efficiency.

Fig. 12 shows the unmodified $\alpha\beta$-axis modulation signals of CSR and the additional damping signals in active damping control are also depicted in Fig. 12(b). As it is shown in Fig. 12, the unmodified modulation signals $m_{c\alpha}$ and $m_{c\beta}$ in both methods are almost the same. Compared with $m_{c\alpha}$ and $m_{c\beta}$, $m_{c\alpha e}$ and $m_{c\beta e}$ are small enough to avoid influencing the normal

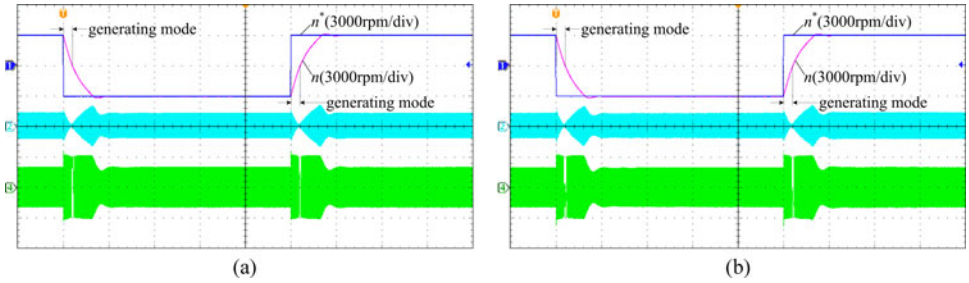

Fig. 14. Speed (n), stator current (i_{oU}) of PMSM, and source current (i_{sA}) when speed reference (n^*) steps between 3000 and −3000 r/min (a) Passive damping control. (b) Active damping control.

operation of IMC, but large enough to suppress the oscillations in source currents.

Figs. 13 and 14 show the experimental results, when the speed reference steps between 3000 and −3000 r/min, necessitating four-quadrant operation of IMC and PMSM. The dq-axis stator currents are calculated by the DSP and output by the DA converter. The three phase stator currents required for control strategy and modulation algorithm come from current sensors. The IMC works in generating mode during the period of speed changing from 3000/−3000 r/min to 0 rpm, while in motoring mode in the rest time. The generating mode lasts about 400 ms, which is 20 cycles of source current period. Since a synchronous generator powering pure resistors acts as the load of PMSM, which generates load torque varying with speed to PMSM, the slop of speed rising and falling is decreasing in the dynamic process. The rising/falling time in two methods is equivalent, which is also true for the speed overshoot, as shown in Table II. Besides, the waveform contours of actual speed, stator current of PMSM, and source current in the proposed strategy are exactly the same with those in passive damping control.

To sum up, the experimental results demonstrate that, the proposed active damping control has the same damping performance with the passive damping control and better filtering performance at source side, maintaining the steady state and dynamic performance of drive control at output side.

VI. Conclusion

The active damping control strategy of MC via modifying input reference currents requires that the amplitude and phase angle are both directly controllable and the top priority of output voltage control must be kept at the same time. In traditional method of generating modulation signals of MC, the expected output voltages are directly synthesized with input voltages, while input currents have to vary passively with output currents. Therefore, this paper makes an improvement to the traditional method by directly synthesizing the input currents with output currents. But the input reference currents are dependent on the expected output active power and, thus, the output voltage control is still preferential in the new method. The new method makes it very easy to realize some control strategies, which require input currents to be directly controllable and the priority of output voltage control to be unaffected, such as the closed-loop control of source currents.

Based on the new method, this paper injects damping signals into input reference currents to completely realize the proposed active damping control strategy. The proposed strategy has the same damping performance with passive damping control strategy and the same filtering performance at input side, maintaining steady state and dynamic performance at output side. No matter the modulation signals are generated from source voltages or capacitor voltages, and what the operation mode of MC is, the proposed strategy is effective. Besides, it is suitable for most of existing modulation algorithms, showing good generality.

Attention should be paid to the calculated dc-link current if both motoring mode and generating mode of MC are required. The minimum absolute value of dc-link current should be limited, in order to avoid negative effects on normal operation of MC due to the division operation. But if MC works in a single mode, the dc-link current can be fixed to the rated value and, thus, solve this problem with only a little effect on damping performance.

References

[1] T. Friedli, J. W. Kolar, J. Rodriguez, and P. W. Wheeler, "Comparative evaluation of three-phase ac-ac matrix converter and voltage dc-link back-to-back converter systems," *IEEE Trans. Ind. Electron.*, vol. 59, no. 12, pp. 4487–4510, Dec. 2012.

[2] J. Kolar, T. Friedli, J. Rodriguez, and P. W. Wheeler, "Review of three phase PWM ac-ac converter topologies," *IEEE Trans. Ind. Electron.*, vol. 58, no. 11, pp. 4988–5006, Nov. 2011.

[3] L. Empringham, J. Kolar, J. Rodriguez, P. W. Wheeler, and J. C. Clare, "Technological issues and industrial application of matrix converters: A review," *IEEE Trans. Ind. Electron.*, vol. 60, no. 10, pp. 4260–4271, Oct. 2013.

[4] J. Rodriguez, M. Rivera, J. W. Kolar, and P. W. Wheeler, "A review of control and modulation methods for matrix converters," *IEEE Trans. Ind. Electron.*, vol. 59, no. 1, pp. 58–70, Jan. 2012.

[5] J. Monteiro, J. F. Silva, S. F. Pinto, and J. Palma, "Linear and sliding-mode control design for matrix converter-based unified power flow controllers," *IEEE Trans. Power Electron.*, vol. 29, no. 7, pp. 3357–3367, Jul. 2014.

[6] L. Zarri, M. Mengoni, A. Tani, and J. O. Ojo, "Range of the linear modulation in matrix converters," *IEEE Trans. Power Electron.*, vol. 29, no. 6, pp. 3166–3178, Jun. 2014.

[7] X. Li, M. Su, Y. Sun, H. Dan, and W. Xiong, "Modulation strategy based on mathematical construction for matrix converter extending the input reactive power range," *IEEE Trans. Power Electron.*, vol. 29, no. 2, pp. 654–664, Feb. 2014.

[8] H.-H. Lee and H. M. Nguyen, "An effective direct-SVM method for matrix converters operating with low-voltage transfer ratio," *IEEE Trans. Power Electron.*, vol. 28, no. 2, pp. 920–929, Feb. 2013.

[9] T. D. Nguyen and H.-H. Lee, "Dual three-phase indirect matrix converter with carrier-based PWM method," *IEEE Trans. Power Electron.*, vol. 29, no. 2, pp. 569–581, Feb. 2014.

[10] X. Liu, P. C. Loh, P. Wang, F. Blaabjerg, Y. Tang, and E. A. Al-Ammar, "Distributed generation using indirect matrix converter in reverse power mode," *IEEE Trans. Power Electron.*, vol. 28, no. 3, pp. 1072–1082, Mar. 2013.

[11] X. Liu, P. C. Loh, P. Wang, and X. Han, "Improved modulation schemes for indirect Z-source matrix converter with sinusoidal input and output waveforms," *IEEE Trans. Power Electron.*, vol. 27, no. 9, pp. 4039–4050, Sep. 2012.

[12] S. Safari, A. Castellazzi, and P. W. Wheeler, "Experimental and analytical performance evaluation of SiC power devices in the matrix converter," *IEEE Trans. Power Electron.*, vol. 29, no. 5, pp. 2584–2596, May 2014.

[13] A. Escobar-Mejia, C. Stewart, J. K. Hayes, S. S. Ang, J. C. Balda, and S. Talakokkula, "Realization of a modular indirect matrix converter system using normally off Sic JFETs," *IEEE Trans. Power Electron.*, vol. 29, no. 5, pp. 2574–2583, May 2014.

[14] A. Trentin, P. Zanchetta, P. W. Wheeler, and J. Clare, "Automated optimal design of input filters for direct ac/ac matrix converters," *IEEE Trans. Ind. Electron.*, vol. 59, no. 7, pp. 2811–2823, Jul. 2011.

[15] J. Andreu, I. Kortabarria, E. Ormaetxea, E. Ibarra, J. L. Martin, and S. Apinaniz, "A step forward towards the development of reliable matrix converters," *IEEE Trans. Ind. Electron.*, vol. 59, no. 1, pp. 167–183, Jan. 2012.

[16] Y. Sun, M. Su, X. Li, H. Wang, and W. Gui, "A general constructive approach to matrix converter stabilization," *IEEE Trans. Ind. Electron.*, vol. 28, no. 1, pp. 418–431, Jan. 2013.

[17] D. Casadei, G. Serra, A. Tani, and L. Zarri, "Effects of input voltage measurement on stability of matrix converter drive system," *Proc. IEE Electr. Power Appl.*, vol. 151, no. 4, pp. 487–497, Jul. 2004.

[18] F. Liu, C. Klumpner, and F. Blaabjerg, "Stability analysis and experimental evaluation of a matrix converter drive system," in *Proc. IEEE 29th Annu.Conf. Ind. Electron. Soc.*, Roanoke, VA, USA, Nov. 2003, pp. 2059–2065.

[19] C. A. J. Ruse, J. C. Clare, and C. Klumpner, "Numerical approach for guaranteeing stable design of practical matrix converter drive systems," in *Proc. IEEE 32nd Annu. Ind. Electron Conf.*, Nov. 2006, pp. 2630–2635.

[20] M. Rivera, J. Rodriguez, B. Wu, J. Espinoza, and C. Rojas, "Current control for an indirect matrix converter with filter resonance mitigation," *IEEE Trans. Ind. Electron.*, vol. 59, no. 1, pp. 71–79, Jan. 2012.

[21] M. Rivera, C. Rojas, J. Rodrıguez, P. Wheeler, B. Wu, and J. R. Espinoza, "Predictive current control with input filter resonance mitigation for a direct matrix converter," *IEEE Trans. Power Electron.*, vol. 26, no. 10, pp. 2794–2803, Oct. 2011.

[22] J. Haruna and J. Itoh, "Behavior of a matrix converter with a feed back control in an input side," in *Proc. Int. Power Electron. Conf.*, 2010, pp. 1202–1207.

[23] I. Sato, J. I. Itoh, H. Ohguchi, A. Odaka, and H. Mine, "An improvement method of matrix converter drives under input voltage disturbances," *IEEE Trans. Power Electron.*, vol. 22, no. 1, pp. 132–138, Jan. 2007.

[24] J. Itoh, I. Sato, A. Odaka, H. Ohguchi, H. Kodachi, and N. Eguchi, "A novel approach to practical matrix converter motor drive system with reverse blocking IGBT," *IEEE Trans. Power Electron.*, vol. 20, no. 6, pp. 1356–1363, Nov. 2005.

[25] J. Haruna and J. Itoh, "Control strategy for a matrix converter with a generator and a motor," in *Proc. 26th IEEE Annu. Appl. Power Electron. Conf.*, 2011, pp. 1782–1789.

[26] P. Wheeler and D. Grant, "Optimized input filter design and low-loss switching techniques for a practical matrix converter," *Proc. IEE Electr. Power Appl.*, vol. 144, no. 1, pp. 53–60, Jan. 1997.

[27] L. Huber and D. Borojevic, "Space vector modulated three-phase to three-phase matrix converter with input power factor correction," *IEEE Trans. Ind. Appl.*, vol. 31, no. 6, pp. 1234–1246, Nov. 1995.

[28] H. Akagi, Y. Kanazawa, and A. Nabae, "Generalized theory of the instantaneous reactive power in three-phase circuits," in *Proc. Int. Power Electron. Conf.*, 1983, pp. 1375–1386.

[29] L. Wei and T. A. Lipo, "A novel matrix converter topology with simple commutation," in *Proc. Rec. IEEE Annu. Ind. Appl. Conf. Meet.*, 2001, vol. 3, pp. 1749–1754.

[30] R. Pena, R. Cardenas, E. Reyes, J. Clare, and P. Wheeler, "Control of a doubly fed induction generator via an indirect matrix converter with changing DC voltage," *IEEE Trans. Ind. Electron.*, vol. 58, no. 10, pp. 4664–4674, Oct. 2011.

[31] X. Wang, H. Lin, B. Feng, and Y. Lyu, "Damping of input LC filter resonance based on virtual resistor for matrix converter," in *Proc. Energy Convers. Congr. Expo.*, 2012, pp. 3910–3916.

[32] D. Casadei, J. Clare, L. Empringham, G. Serra, A. Tani, A. Trentin, P. Wheeler, and L. Zarri, "Large-signal model for the stability analysis of matrix converters," *IEEE Trans. Ind. Electron.*, vol. 54, no. 2, pp. 939–950, Apr. 2007.

[33] P. Cardenas, R. Pena, G. Tobar, J. Clare, P. Wheeler, and G. Asher, "Stability analysis of a wind energy conversion system based on a doubly fed induction generator fed by a matrix converter," *IEEE Trans. Ind. Electron.*, vol. 56, no. 10, pp. 4194–4206, Oct. 2009.

Jiaxing Lei (S'14) was born in Dazhou, China, 1991. He received the B.S. degree from the Nanjing University of Aeronautics and Astronautics, Nanjing, China, in 2012, where he is currently working toward the Ph.D. degree.

His main research interests include matrix converters and its applications in aerospace power system.

Bo Zhou was born in Wenzhou, Zhejiang Province, China, in 1961. He received the B.S. degree from Zhejiang University, Hangzhou, China, in 1983, the M.S. degree from Chongqing University, Chongqing, China, in 1986, and the Ph.D. degree from the Nanjing University of Aeronautics and Astronautics (NUAA), Nanjing, China, in 2000.

He worked with the Nanjing University of Aeronautics and Astronautics. He is currently a Professor with the College of Automation Engineering, NUAA, and is the Director of the Jiangsu Key Laboratory of New Energy Generation and Power Conversion. His research interests include power converter, electrical machine driving systems, and renewable power systems.

Prof. Zhou received the State Technological Invention Second-Class Award in 2009, the Geneva International Invention gold award in 2011, and the Defense Technological Invention first prize in 2008.

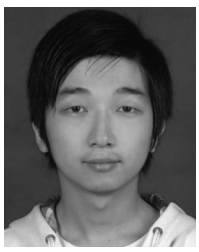

Xianhui Qin was born in Beijing, China, in 1988. He received the B.S. degree from the Nanjing University of Aeronautics and Astronautics, Nanjing, China, in 2009, where he is currently working toward the Ph.D. degree.

His main research interests include aeronautic static power conversion, and the design and control technology for practical matrix converters.

Jiadan Wei (M'10) was born in Danyang, Jiangsu Province, China, in 1981. He received the B.S. and Ph.D. degrees in electrical engineering from the Nanjing University of Aeronautics and Astronautics (NUAA), Nanjing, China, in 2003 and 2009, respectively.

He is currently an Associate Professor at the College of Automation Engineering, NUAA. His research interests include the power electronics, motion control system, and renewable power systems.

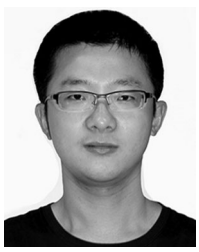

Jinliang Bian was born in Nantong, China, in 1990. He received the B.S. degree from the Nanjing University of Aeronautics and Astronautics, Nanjing, China, in 2013, where he is currently working toward the M.S. degree.

His main research interests include matrix converters and its applications in aerospace power system.